SUPPORTING INFORMATION

Tunable surface structuration of silicon by metal assisted chemical etching with Pt nanoparticles under electrochemical bias

Encarnación Torralba[‡,†], Sylvain Le Gall[‡,‡], Raphaël Lachaume[‡], Vincent Magnin[§], Joseph Harari[§], Mathieu Halbwax[§], Jean-Pierre Vilcot[§], Christine Cachet-Vivier[†], Stéphane Bastide*[†]

[†] Institut de Chimie et des Matériaux Paris-Est, CNRS, Université Paris-Est, 2-8 rue Henri Dunant, 94320 Thiais, France

[‡] Group of electrical engineering – Paris, UMR CNRS 8507, Centrale Supélec, Univ. Paris-Sud, Université Paris-Saclay, Sorbonne Universités, UPMC Université Paris 06, 3 & 11 rue Joliot-Curie, Plateau de Moulon 91192 Gif-sur-Yvette CEDEX, France

[§] Institut d'Électronique, de Microélectronique et de Nanotechnologie, UMR CNRS 8520, Université de Lille 1 - Sciences et Technologies, Avenue Henri Poincaré, CS 60069, 59652 Villeneuve d'Ascq cedex, France

* To whom correspondence should be addressed. Phone:+33 01 49 78 13 30, E-mail: bastide@icmpe.cnrs.fr

S1. Nanoparticle size distribution

The size distribution of Pt NPs obtained on p-type (100) Si surfaces by immersion in an aqueous solution of 1 mM H_2PtCl_6 and 90 mM HF for 120 s is presented in Figure S1. The feret diameter has been measured from SEM images processing using the software ImageJ. The average diameter is 50 nm and the Pt coverage 12%.

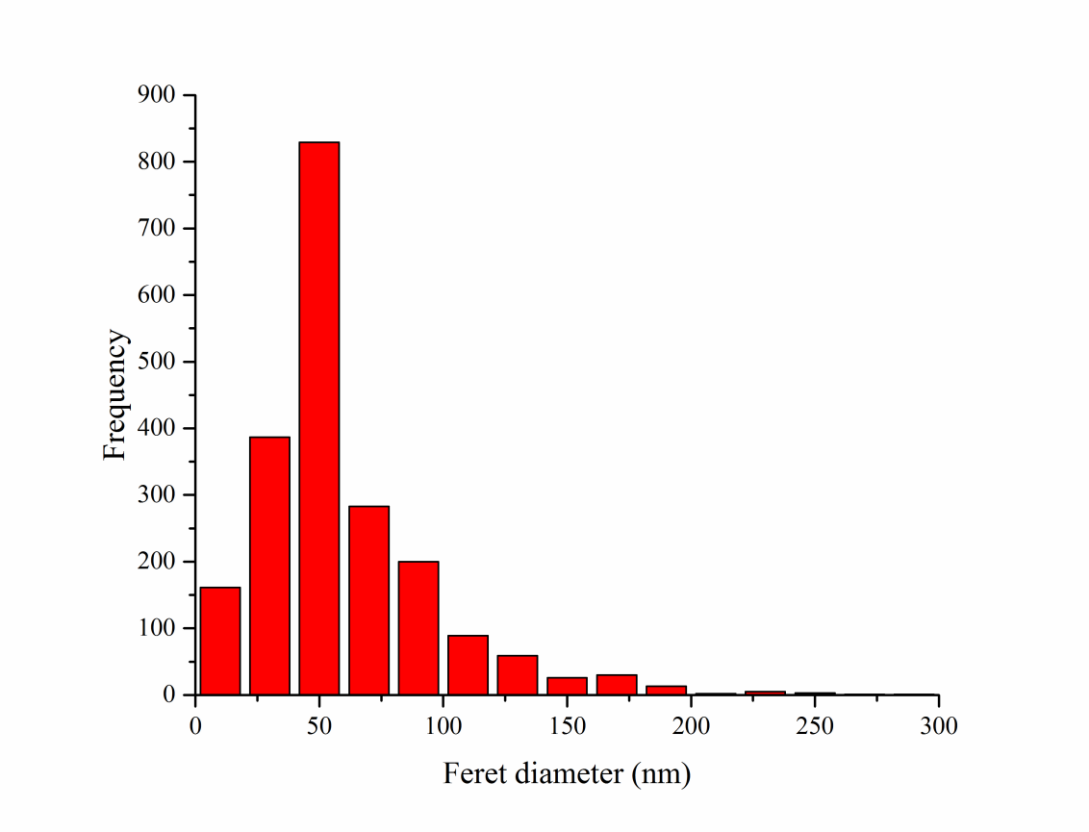

Figure S1. Feret diameter of the Pt NPs obtained by electroless Pt deposition in 1 mM H_2PtCl_6 and 90 mM HF for 120 s, as deduced from SEM observations and image processing with the software ImageJ.

S2. Experimental Mott-Schottky plots

In the depletion regime, the capacitance C of a metal/semiconductor (Schottky) junction can be described by the Mott-Schottky (MS) equation:[1]

For p-type
$$\frac{1}{C^2} = \frac{2}{\varepsilon_r \varepsilon_0 A^2 e N_A}\left[-\left(V - V_{fb,p}\right) - \frac{k_B T}{e}\right] \quad \text{(S1)}$$

For n-type
$$\frac{1}{C^2} = \frac{2}{\varepsilon_r \varepsilon_0 A^2 e N_D}\left[\left(V - V_{fb,n}\right) - \frac{k_B T}{e}\right] \quad \text{(S2)}$$

where N_A and N_D represent the doping densities for p-type and n-type respectively, ε_r is the relative permittivity of the semiconductor, ε_0 the vacuum permittivity, A the electrode surface area, V the applied potential, $V_{fb,p}$ and $V_{fb,n}$ the flat-band potentials for p and n-type, e the elementary charge, k_B the Boltzmann constant and T the working temperature.

The slope and the ordinate of the linear MS plots allow the experimental determination of the flat-band potential and doping density of a given semiconductor, two important parameters to describe its physical properties and required to perform the band bending simulations depicted in this work.

Figures S2(a) and S2(b) show the MS plots obtained respectively for platinized and bare n-type and p-type Si in contact with a solution of HF at 3.63 M. Although several frequencies were applied giving comparable doping densities and flat band potential values, only the MS plots measured at 50 kHz are shown for the sake of clarity.

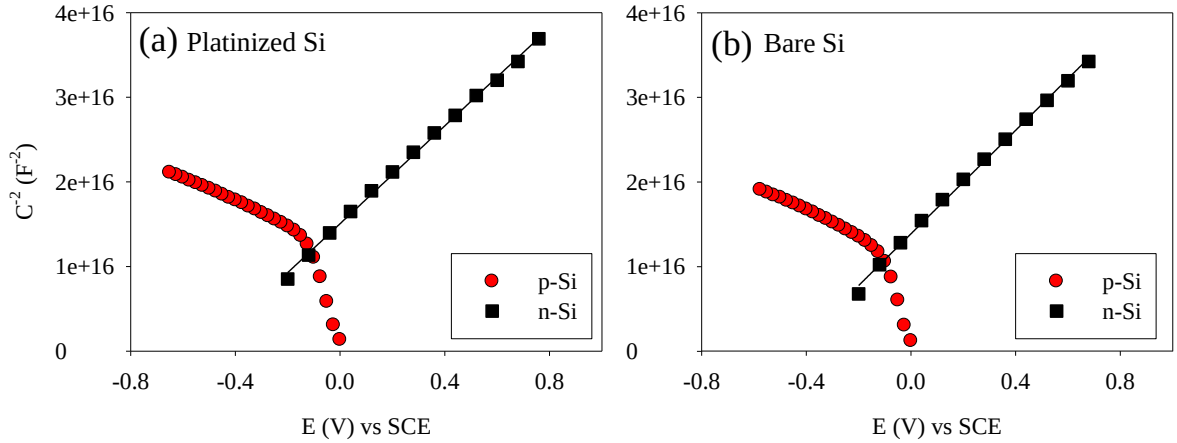

Figure S2. MS plots ($1/C^2$ vs E) recorded for platinized (a) and bare (b) Si(100), p and n doped (red circles and black squares, respectively) in contact with a solution of HF at 3.63 M at a frequency of 50 KHz. Solid lines represent the linear fittings. All measurements were performed in the dark under Ar atmosphere. The resistivity of both p and n type samples was 1-3 Ωcm.

The doping densities calculated from MS plots are $N_D = 2.3\times10^{15}$ cm^{-3} and $N_A = 5.6\times10^{15}$ cm^{-3} (Table S1), in good agreement with the resistivity ranges indicated by the supplier: $1.6 – 5.0\times10^{15}$ cm^{-3} for n-type Si and 4.7×10^{15} - 1.5×10^{16} cm^{-3} for p-type Si.

It is well known that V_{fb} measurements of Si in HF from MS plots are only reliable with n-type Si[2]. In the case of p-type Si, deviations in flat band potential measurements are usually observed. According to the literature, a partial compensation or neutralisation of acceptors occurs at the surface due to the incorporation of hydrogen at large negative potentials and/or under light[2]. Consequently, $V_{fb,p}$ was calculated in an indirect way, by using $V_{fb,n}$ and N_D obtained from the MS plots of n-type Si and applying the following expression:[2]

$$V_{fb,p} = V_{fb,n} + \frac{1}{e}\left[E_g + k_B T \ln\left(\frac{N_D N_A}{N_c N_v} \right) \right] \qquad \text{(S3)}$$

where E_g is the band gap of Si, $N_c = 2.70\times10^{19}$ cm^{-3} and $N_v = 1.04\times10^{19}$ cm^{-3} the effective density of states in the conduction and valence band, respectively. The calculated values are given in Table S1.

Table S1. Doping densities, OCP and V_{fb} determined experimentally from the MS plots of bare and platinized Si (p and n-type) in a 0.5 M HF aqueous solution under Ar bubbling and in the dark.

	Bare n-Si	**Pt n-Si**		**Bare p-Si**	**Pt p-Si**
$N_{D,A}$ (cm^{-3})	2.3×10^{15}	--		5.6×10^{15}	--
OCP (V vs. SCE)	-0.26	-0.28		-0.36	-0.30
V_{fb} (V vs. SCE)	-0.50	-0.56		0.18	0.13

From bare n-Si $V_{fb,n}$, we can estimate the experimental effective work function (*vs.* vacuum level) of the electrolyte W_{EL} using the following expression:

$$W_{EL} = \chi_{Si} - \frac{k_B T}{e} \ln\left(\frac{N_D}{N_c}\right) - eV^0_{fb,n} \quad \text{(S4)}$$

where χ_{Si} =4.05 eV is the electronic affinity of Si and $V^0_{fb,n}$ is the equilibrium flat band potential for which the energy reference is the equilibrium Femi-Level. $V^0_{fb,n}$ can be deduced from the experimental $V_{fb,n}$ by subtracting the measured OCP value (here $V^0_{fb,n}$ = -0.24 V). Using equation (S4), we find W_{EL}=4.53 eV, which is compatible with values from the literature.[2,3] This parameter will be fixed to W_{EL}=4.5 eV in the simulations of the band bending.

S3. Band Bending Simulations

The modelling has been performed using the commercial TCAD software Atlas from Silvaco© [4]. This simulator solves the physical equations governing the electrostatics (Poisson, electro-neutrality) and the transport of e^- and h^+ (drift-diffusion) self-consistently on a 2D mesh.

S3.1. Design of the Pt NP/Si/Electrolyte structure

Figure S3 shows a scheme of the Electrolyte/Pt NP/p-Si structure used for the simulations displayed in Figure 5(a-d). This structure comprises a 100 µm thick p-type Si substrate doped with $N_A = 6\times10^{15}$ cm^{-3}. The Si substrate is fitted with three metallic electrodes on top corresponding respectively to the Electrolyte, the Pt NP and again the Electrolyte (both Electrolyte electrodes being short-circuited). The total width (x-axis) of the structure is 0.1 µm. The Pt NP contact is positioned at the middle of the structure and covers 12% of the entire width. To avoid a short-circuit between the Electrolyte and the Pt NP electrodes, the latters are separated by a space of 1 nm. A voltage can be applied between the Electrolyte (-) and Pt (+) electrodes to give account of the potential distribution and current flow during MACE (*i.e.* oxidation of Si at the level of the Electrolyte coupled to the reduction of H_2O_2 at the level of Pt). An identical structure with a n-type Si substrate (N_D= 3×10^{15} cm^{-3}) has also been modelled.

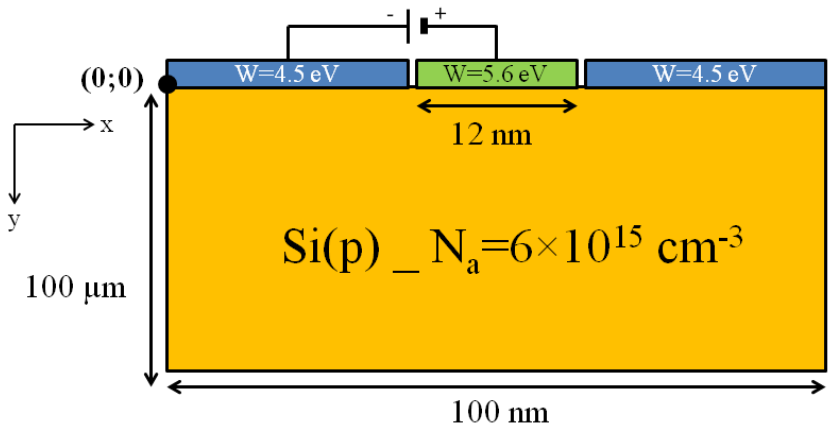

Figure S3. Structure used for the band bending modelling of the Pt NP/Si/Electrolyte junction at equilibrum and under an applied polarization mimicking the MACE process.

S3.2 Simulation of Mott-Schottky plots

In order to adjust the modelling with the real experimental conditions, it was necessary to set the work functions for the Electrolyte and the Metal. This was done by comparing the behavior of the modelled and experimental Electrolyte/Si (Pt) junctions through their MS plots (*i.e.* obtained with SILVACO and experimentally). The best agreement between simulations and experiments in terms of flat band potentials is reported in the Table S2.

Table S2. Flat band potentials obtained from experimental MS plots (0.5 M HF, Ar, dark) and simulated MS plots (with the structure of Figure S3) for bare and platinized Si (p and n-type).

	Bare n-Si	**Pt n-Si**		**Bare p-Si**	**Pt p-Si**
Experimental V_{fb} (V) *	-0.24	-0.28		+0.54	+0.43
Simulated V_{fb} (V) *	-0.22	-0.34		+0.50	+0.41

** In the simulations, V_{fb} values are given with respect to the Fermi level of the Metal or Electrolyte (at equilibrium), whereas in experiments, the 0 V reference is the SCE potential. To compare V_{fb} in both systems, the experimental values are referenced to the measured OCP (equivalent to the Fermi level of the Metal or Electrolyte in the simulations). The OCP can however slightly fluctuate with time, for instance because of changes in the solution (O_2 concentration) or in the surrounding light.*

In this set of data, the Electrolyte is modelled as a metal with an effective work function W_{EL}=4.5 eV. The doping densities of bare n-type and p-type Si are $N_D = 3\times10^{15}$ cm^{-3} and $N_A = 6\times10^{15}$ cm^{-3}. In the case of platinized Si, the Pt work function used is W_{Pt} = 5.6 eV, in agreement with the literature[5], and the Pt coverage is 12% as deduced from SEM observations.

The MS plots and V_{fb} values calculated from the modelled structure and measured experimentally are in very good agreement. This indicates that the band bending modelling provides reliable information and can be used with confidence to explain the Pt based MACE process.

S3.3 "*In situ*" modelling of MACE with Pt NPs

Figure S4 represents a close view of the simulated 2D profiles in Si and around the Pt NP once it has sunk into the substrate. The Pt NP has a size of 50 nm, is buried at the bottom of a 1 µm deep mesopore and is polarized at +0.2 V vs. the Electrolyte.

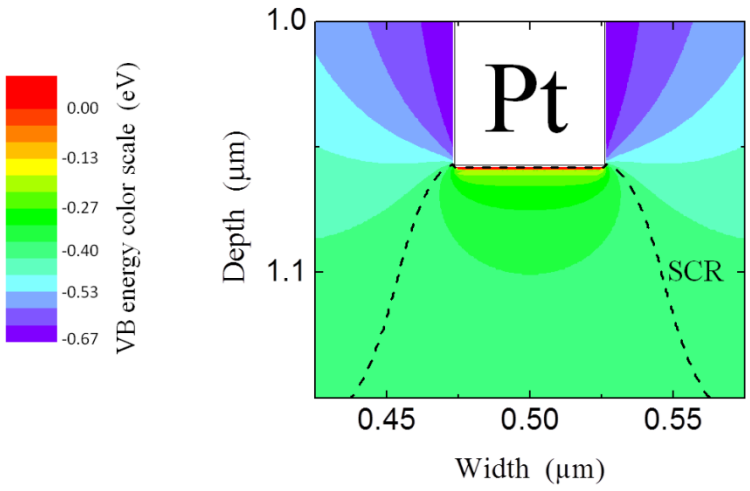

Figure S4. Close view of the "in situ" modelling of MACE at the level of a Pt NP (50 nm) that has digged a pore of 1 µm. The NP is polarized at +0.2 V vs. the Electrolyte.

S4. MACE of (111) oriented Si with Pt NPs

Figure S5 shows two SEM images taken at 45° (unpublished results) of (a) p-type (111) oriented Si and (b) p-type multycristalline Si after MACE in HF/H_2O_2 ($\rho = 0.5$) with Pt NPs, followed by dissolution of porous Si in HF/HNO_3 to reveal the macropores. There is a clear dependance of the preferred etching directions followed by Pt NPs on the crystallographic orientation. With (111) Si, the macropores are oriented along the <100> directions. With multicrystalline Si, two adjacent grains exhibit macropores with very disctinct orientations on each side of the grain boundary.

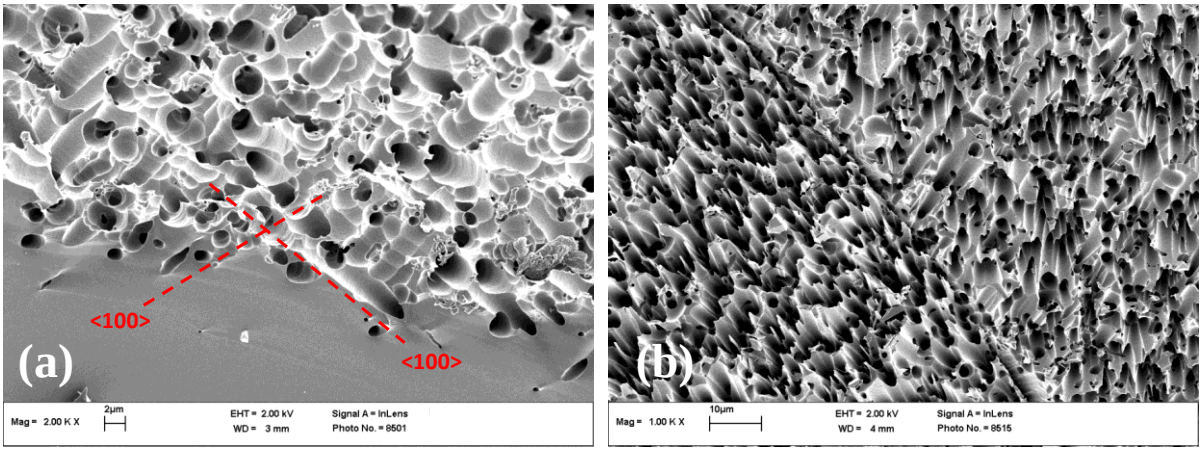

Figure S5. SEM image of (111) p-type Si (a) and multicrystalline p-type Si (b) after MACE in HF/H_2O_2 ($\rho = 0.5$) with Pt NPs and dissolution of porous Si in HF/HNO_3.

References

(1) Michalak, D. J.; Gstrein, F.; Lewis, N. S. Interfacial Energetics of Silicon in Contact with 11 M NH_4 F(aq), Buffered HF(aq), 27 M HF(aq), and 18 M H_2SO_4. *J. Phys. Chem. C* 2007, *111* (44), 16516–16532.

(2) Ottow, S.; Popkirov, G. S.; Föll, H. Determination of Flat-Band Potentials of Silicon Electrodes in HF by Means of Ac Resistance Measurements. *J. Electroanal. Chem.* 1998, *455* (1–2), 29–37.

(3) Zhang, X. G. *Electrochemistry of Silicon and Its Oxide*, 1st ed; Springer International Publishing AG: Switzerland, 2001.

(4) Atlas User's Manual, Device Simulation Software. Silvaco International 2006.

(5) Michaelson, H. B. The Work Function of the Elements and Its Periodicity. *J. Appl. Phys.* 1977, *48* (11), 4729–4733.